Integration of a dual-band IR data acquisition system using low-cost PV320 cameras

Joseph P. Havlicek[a], Chuong T. Nguyen[a], Guoliang Fan[b], and Vijay B. Venkataraman[b]

[a]University of Oklahoma, Norman, OK, USA
[b]Oklahoma State University, Stillwater, OK, USA

ABSTRACT

The Electrophysics PV320 is a broadband thermal imaging system with several attractive features including low cost (about USD 25K including optics and software), small size, uncooled operation with a BST sensor array, spectral response from 0.6 to 14 μm, easily interchangeable warm optics, and on board USB 2.0 digital video output. In this paper we describe the technical challenges that were involved in integrating together two copies of the PV320L2Z camera variant to create an experimental dual-band IR data acquisition system for measuring targets, backgrounds, and clutter. The PV320 manufacturer-supplied software includes a user friendly, all-in-one application as well as software development kits providing camera control routines that are callable from C++, Visual Basic, and LabView. While this software works well for operating a single PV320 camera, it does not provide any direct support for simultaneously imaging with multiple cameras. The main technical issues are that the base software driver can connect to only one camera at a time and that multiple instances of the driver cannot be loaded simultaneously. Therefore, to achieve our goal of acquiring dual-band IR signatures, it was necessary to program a custom distributed algorithm capable of running two copies of the driver simultaneously on two separate computers with one PV320L2Z connected to each.

Keywords: Dual-band infrared, PV320 camera, longwave infrared, midwave infrared, color fusion

1. INTRODUCTION

Military interest in dual-band infrared imaging systems has grown steadily over the past 15 years. The thermal signatures of targets and backgrounds are typically a strong function of wavelength, and this fact can be leveraged to achieve improved target detection, clutter rejection, and discrimination between targets and backgrounds by jointly processing dual-band sensor measurements,[1–7] whether at the pixel or feature level. Since atmospheric transmittance through clear air, water vapor, and, e.g., smoke are also wavelength dependent, dual-band systems can provide improved target detection in a variety of battlefield ambient conditions.[1,5,8] In addition to its obvious utility in providing input to advanced automatic or assisted target recognition (ATR) systems, the imagery from dual-band sensors can also be fused to obtain displays suitable for direct human consumption that have the potential to dramatically enhance battlefield situational awareness and improve performance in surveillance applications while simultaneously reducing the workload on military crews.[3,5]

Despite the fact that the potential of multi-color thermal sensors for improving performance in a variety of military systems has been well established, a systematic theory for jointly processing and fusing dual-band data has yet to emerge. One of our main goals has been to investigate the application of modulation domain signal processing techniques[9,10] in this problem domain. However, our efforts in this regard have been significantly impeded by the general paucity of dual-band IR data available in the public domain. Consequently, it became necessary to construct a low cost data acquisition system capable of delivering reasonably high-quality dual-band measurements. In this paper, we describe the details of the system design and the rather significant software engineering efforts that were required to integrate it and make it operational. The basic system components are described in Section 2, including the rationale behind our selection of camera technology. The software development effort that was required to integrate the system is detailed chronologically in Section 3. The main technical challenges in this area arose from the fact that the selected cameras (including their device drivers

This work was supported in part by the U.S. Army Research Laboratory and the U.S. Army Research Office under grant W911NF-04-1-0221. Author E-mail: joebob@ou.edu, chuong@ou.edu, guoliang.fan@okstate.edu, vj2181@yahoo.com.

Infrared Technology and Applications XXXII, edited by Bjørn F. Andresen, Gabor F. Fulop, Paul R. Norton,
Proc. of SPIE Vol. 6206, 62061U, (2006) · 0277-786X/06/$15 · doi: 10.1117/12.666140

(a)
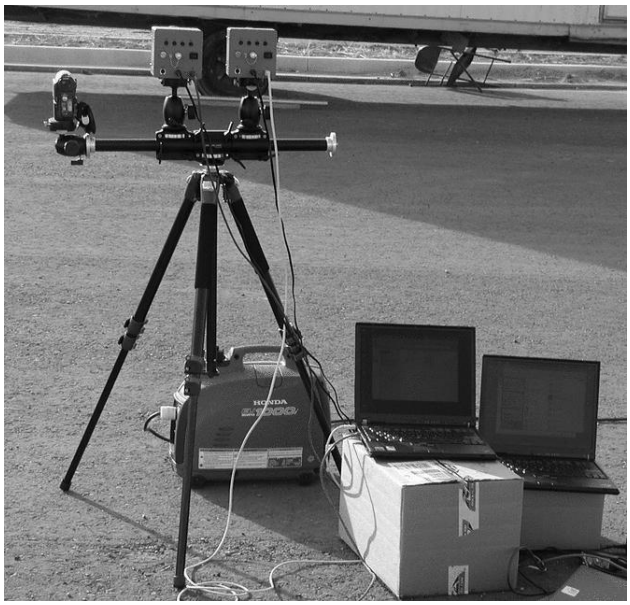

(b)

Figure 1. Portable, low-cost dual-band infrared data acquisition system. (a) Sensor array including two PV320L2Z broadband cameras with warm filters limiting the spectral response to 3 – 5 μm and 8 – 12 μm. (b) Rear view of system showing camera electrical interfaces, control computers, and portable generator. The generator provides about four hours of field operation without AC power.

and software) were not designed to operate in a dual-band mode. Examples of dual-band imagery acquired with the system and data fusion between the midwave and longwave infrared bands are given in Section 4. Several issues regarding the system sensitivity and ambient imaging conditions are discussed in Section 5. Finally, the summary and conclusions are reserved for Section 6.

2. SYSTEM HARDWARE COMPONENTS

Consistent with the work reported in Refs. 1, 5–7, we decided early on to focus our attention on the 3–5 μm midwave infrared (MWIR) and 8–12 μm longwave infrared (LWIR) atmospheric transmission bands. With the advent of quantum well infrared photodetector (QWIP) and mercury cadmium telluride (HgCdTe) detector arrays capable of simultaneously delivering spatially and temporally registered, high-quality MWIR and LWIR frames, these bands have been the subject of considerable recent interest. However, these detector technologies are not readily available at a reasonable cost for unclassified research. More conventional technologies including cryogenically cooled InSb or HgCdTe detector arrays operated in dual cameras or in a single camera with a filter wheel were also cost prohibitive for this project.

With cost as the primary driving factor, we ultimately selected a pair of Electrophysics PV320L2Z uncooled broadband cameras, which are shown in Fig. 1(a). Each camera is equipped with a 320 $\times$ 240 focal plane array (FPA) of pyroelectric barium strontium titanium (BST) detector elements stabilized by a thermoelectric cooler for operation in ambient temperatures from -20° C to 50° C. The spectral response is from 0.6 to 20 μm. The camera provides on board non-uniformity correction (NUC) and a defeatable automatic gain control mechanism. Electrical interfaces are located on the back of the camera housing, as depicted in Fig. 1(b). NTSC or PAL composite video is available through a BNC connector, while a USB 2.0 port provides 12-bit digital video as well as communication with the on board camera controller. The rear panel also provides a four-button user interface that supports basic camera configuration and operation of the composite video port without external software. The frame rate is approximately 30 Hz. We fitted each camera with a 50 mm $f/1.0$ lens providing a field of view of $18^\circ \times 13.5^\circ$. Warm filters are placed between the lens and detector to limit the spectral response. Typically, we operate one camera in the 3–5 μm MWIR band and the other in the 8–12 μm LWIR band. Including optics and software, the cost of these cameras was approximately USD 25K each.

The complete data acquisition system is shown in Fig. 1. The sensor array appears in Fig. 1(a) and includes the two PV320L2Z and a visible wavelength digital camcorder. As shown in Fig. 1(b), system control is via two laptop computers under the Microsoft Windows operating system, which are configured as master and slave through a TCP/IP connection. The portable generator shown in Fig. 1(b) provides approximately four hours of continuous field operation.

3. SOFTWARE AND SYSTEM INTEGRATION

Three main external software packages are available from the manufacturer for digital video acquisition and comprehensive control of the PV320L2Z. There is a stand alone graphical user interface (GUI) based program that supports a variety of image and video acquisition modes, as well as a number of image processing and analysis functions. In addition, there are software development kits that provide application program interfaces (API's) callable from Microsoft Visual C++ or Visual Basic or from National Instruments LabView. Each API contains a set of approximately 45 predefined high-level functions hard coded and encrypted in a dynamic link library (DLL). Functions are provided, e.g., for license server and connection management, image and video acquisition, setting and resetting the autoexposure controls, and manually controlling the video sensitivity, gain, and level.

The first problem that emerged in integrating the system was that the license server, which is required for any acquisition of digital imagery or video, is inherently incapable of supporting more than one camera at any given time. This fact immediately ruled out the possibility of using the manufacturer's GUI-based stand alone software in this system. Therefore, we elected to develop a custom control software using the C++ API. Early testing revealed a second difficulty: multiple instances of the license server cannot be run simultaneously on a single platform. Our initial design concept was for a single control computer to run the entire data acquisition system with the two cameras being connected to two individual USB 2.0 ports. However, this second problem necessitated a design revision incorporating a second computer so that two instances of the license server could be run independently on separate platforms for the two cameras.

In the revised system concept, one computer functions as master while the other functions as slave. This required the development of separate software applications for the master and slave. The master and slave communicate at 1.0 Gbps through a cross-over cable via a dedicated TCP/IP socket. System control is effected through the master, which manages data acquisition for one camera while simultaneously instructing the slave to acquire data from the second camera. We designed a GUI-based control application using the Microsoft Foundation Classes (MFC) that was successful in acquiring dual-band imagery. However, maintaining temporal synchronization between the frames acquired by the two cameras quickly emerged as a major problem with this approach. Although the first few frames would typically be well synchronized, temporal registration was invariably lost within the first few seconds of video acquisition. Over a 10 second video acquisition interval, we commonly observed temporal misalignments as large as 100 to 200 μs by the end of the sequence. Attempts to correct the temporal registration by inserting timing loops to slow down the faster computer were unsuccessful. Because of the intensive low-level I/O load between the USB controller, main memory, and disk, the actual frame rate that can be maintained in practice using the API calls is strongly dependent on the particular hardware configuration and BIOS level of each computer. Even using identical computers, synchronization could not be maintained due to random, unpredictable background tasks being performed by the operating system and by competing threads.

Near perfect temporal registration was ultimately achieved in the final design revision, which implemented lock-step processing between the master and slave computers. A block diagram of the software control flow is shown in Fig. 2. During initialization, the server application is first started on the master computer. It opens a port for communication by calling a Winsock wrapper library in Microsoft Visual C++ MFC. The client application is then initiated on the slave machine. The slave makes a request for connection by sending a hard-coded IP address and the current port number. When this request is accepted by the master, a TCP/IP socket is created that enables the master to issue commands to the slave and receive service requests from the slave. From this point forward, the master dictates all activities of the system. For each action that is to be performed, the master constructs a command in a text string which is sent to the slave. The master and slave then execute the command simultaneously by making API calls to access their respective cameras.

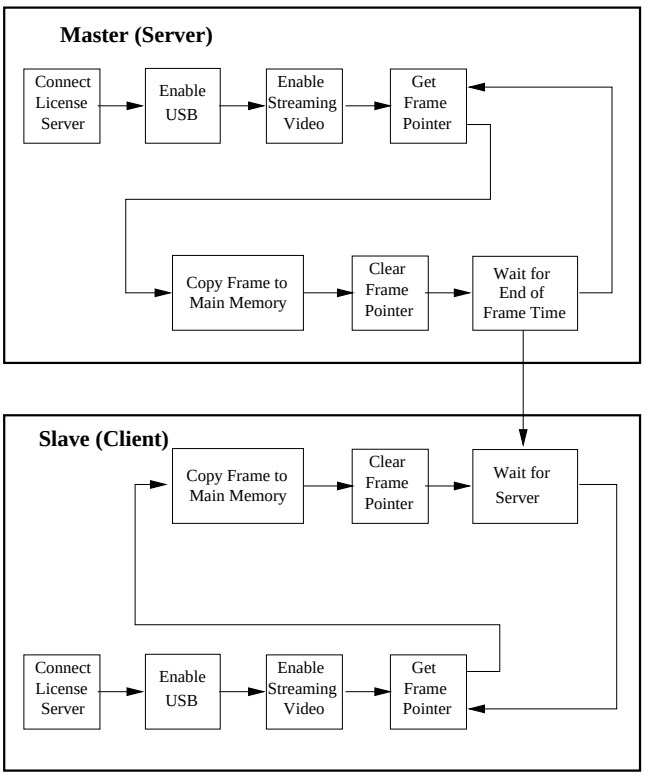

Figure 2. Software block diagram depicting lock-step control between the master and slave computers. After each frame is acquired, the slave waits until the frame time counter at the master has expired. Both computers then proceed simultaneously with acquisition of the next frame.

To begin data acquisition, both computers establish a connection to their respective license servers and pass in a desired license number. The license server compares this to the license number stored in ROM on board the camera. Provided that the licenses match, the camera establishes a control connection to the application program through the USB port. The API call `IR_InitBulkTransferUSB` is then executed by both computers to open the USB interfaces for data transfers. Memory buffers for storing IR frames are then allocated on each computer and associated with corresponding buffers on board the cameras by executing the API call `IR_EnableVideoStreaming`. At this point, the system is ready to acquire dual-band imagery. The master and slave computers then enter a lock-step loop that is controlled by the master through the TCP/IP connection. One pair of MWIR and LWIR frames is acquired on each iteration of the loop. The master and slave simultaneously issue an `IR_GetPixelFramePointer` API call to their respective cameras. This initiates a USB 2.0 transfer of one frame of data from the camera memory buffer to the corresponding buffer in the computer. Each computer independently issues an `IR_ClearPixelFramePointer` API call when the transfer completes to release the camera buffer. After the buffer is released in the camera connected to the master computer, the master enters a delay loop until the end of the 30 ms frame time is reached. The master then initiates the next iteration of the loop by commanding both computers to issue another `IR_GetPixelFramePointer` API call, which begins the data transfer for the next pair of MWIR and LWIR frames. When the predetermined number of dual-band frame pairs have been acquired, the loop terminates, both computers issue an `IR_EnableVideoStreaming` API call to disable the USB connection, and the contents of the memory buffers are written to disk files.

A similar but less rigorous procedure is used to acquire frames for display in order to set the focus and video display parameters of the cameras prior to actually acquiring temporally registered dual band frames. In this mode, the software control flow is as depicted in Fig. 2, but lock step processing between the master and slave is not enforced and data is not written to disk. Instead, each frame is processed with a global gain and bias, truncated to eight bits, and dumped to the display driver. The server and client applications provide GUI

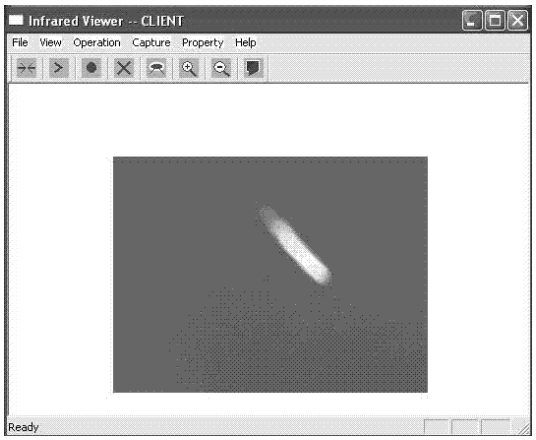

Figure 3. Screen shot of the graphical user interface (GUI) of the client application which runs on the slave computer. The main window depicts the imagery that is being acquired from the camera. Pulldowns and dialogs are provided for all of the camera control functions as well as for controlling communications between the master and slave computers.

dialogs for setting the color map, enabling or disabling autoexposure control on board the camera, adjusting the sensitivity, level, and gain, setting the zoom, and enabling frame averaging. Because of the additional processing load associated with scaling the data for display and handling the user interface, it is impossible to maintain temporal registration between the MWIR and LWIR cameras in this mode. A screenshot of the GUI for the client application is given in Fig. 3.

4. IMAGERY AND DATA FUSION EXAMPLES

Two dual-band frame pairs acquired with the system early in the afternoon during May, 2005, are shown in Fig. 4. The ambient temperature was above 32° C and the air was clear. The 8–12 μm LWIR frames are shown in Fig. 4(a) and (d), while the corresponding temporally registered 3–5 μm MWIR frames are shown in Fig. 4(b) and (e). The scene is of a corporate class jet aircraft preparing for taxi on the tarmac at the regional airport in Stillwater, OK. These examples demonstrate the dramatically different views of a scene that can be obtained by dual-band thermal imaging. Whereas the aircraft empenage is prominent in the LWIR image of Fig. 4(a), it is barely visible in the MWIR image of Fig. 4(b). Conversely, the engine plume dominates Fig. 4(b) but is virtually invisible in Fig. 4(a). Likewise, a bright midwave reflection from the cockpit window dominates the MWIR view of Fig. 4(e), but is utterly absent in the LWIR frame of Fig. 4(d). The passengers, who are almost invisible in Fig. 4(e), are imaged with good detail and are clearly visible in Fig. 4(d).

These two frames were registered to the nearest integer pixel translation and dual band fusion was performed. The extremes of each pair were equalized and then the equalized LWIR and MWIR frames were simply added. The results are given in Fig. 4(e) and (f), where the salient features from each band are evident in the fused imagery. In particular, the engine plume, empinage, and landing gear can all be seen in Fig. 4(c). Similarly, the passengers as well as the midwave cockpit reflection are all clearly visible in Fig. 4(f).

The example given in Fig. 5 shows a sport utility vehicle imaged in the late afternoon during, May, 2005. The vehicle was in motion during the acquisition. The ambient conditions were similar to those of the examples in Fig. 4, but the range to target was significantly larger. The LWIR frame is given in Fig. 5(a), where the engine signature is clearly visible along with some significant clutter structure. Fig. 5(b) shows the MWIR frame, which is of somewhat lower quality than the frames shown in Fig. 4(b) and (e). This is attributed mainly to the longer range to target and the relatively attenuated radiation incident on the detector with the 3 – 5 μm midwave filter in place compared to the 0.6 – 14.0 μm broadband operating environment to which the PV320L2Z is best suited. In fact, the PV320L2Z spectral response is quite nonlinear in the 3 – 5 μm band and exhibits a local minimum of 20% standard response at approximately 5 μm. Temporal aliasing artifacts are also visible in Fig. 5(b), which seem to be typical of the API and also occur when the manufacturer's stand alone program is used. Nevertheless, the engine signature stands out much better against the clutter in Fig. 5(b) than in the LWIR frame of Fig. 5(a).

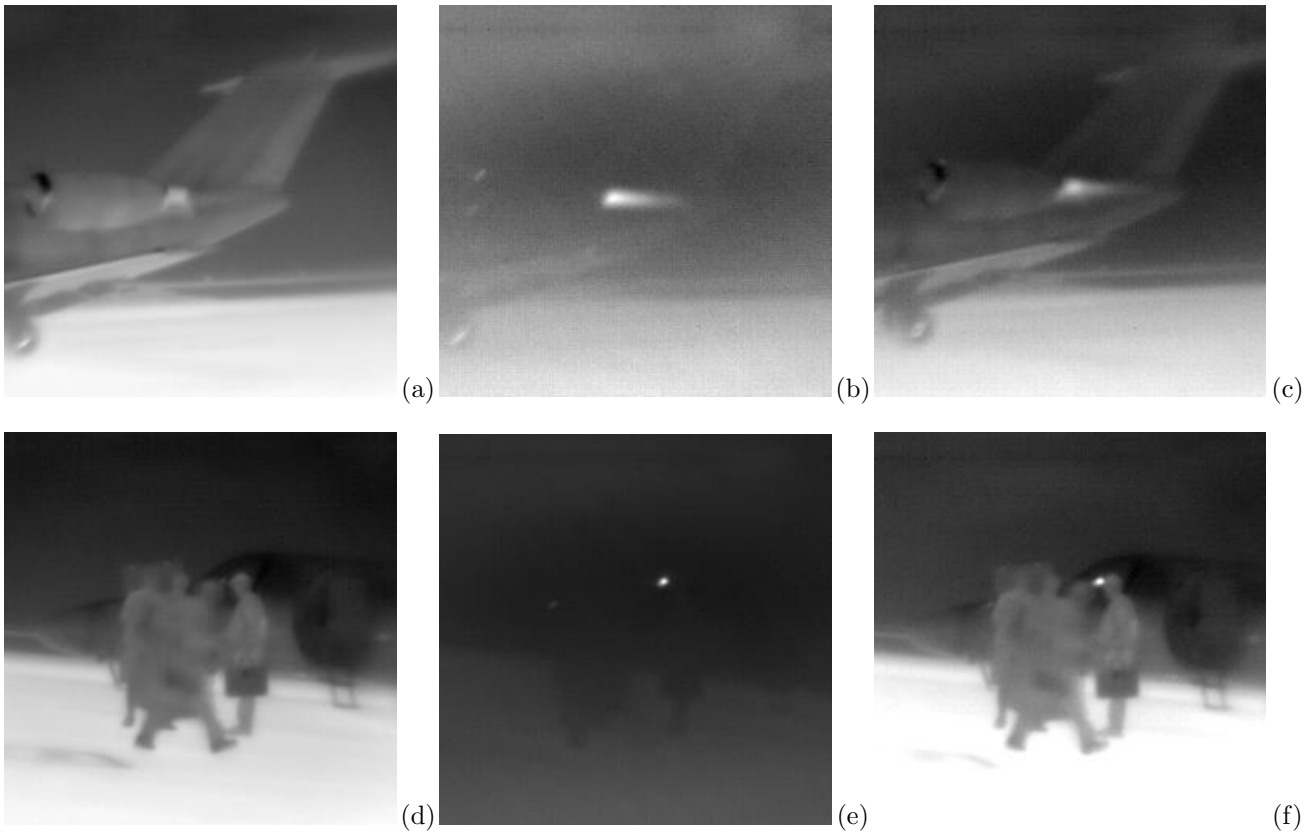

Figure 4. Dual-band imagery and fusion examples. (a) Empinage and engine in the LWIR band. (b) Empinage and engine in the MWIR band. (c) Dual-band fusion result obtained by summing (a) and (b) after spatial registration and equalization. (d) Passengers and cockpit in the LWIR band. (e) Passengers and cockpit in the MWIR band. (f) Dual-band fusion result obtained by summing (d) and (e) after spatial registration and equalization.

The LWIR and MWIR frames of Fig. 5 were fused using the spectral correlation (linear whitening) filter given in Eq. (1) of Ref. 11. Intuitively, this filter subtracts one band from the other using a separate weight for each pixel, where the weight is an estimate of the correlation between bands computed in a spatially local neighborhood about the pixel. In this context, one band is usually regarded as primary and the other as reference. The assumption is that the target signatures lie mostly in the primary band, whereas the clutter and backgrounds admit correlated signatures in both bands. To the extent that this assumption is valid, subtracting the reference band from the primary band with an appropriate local weighting tends to reduce the clutter variance. When there is sufficient correlation between the clutter signatures in the two bands, the effect can be dramatic. Here, we have taken the MWIR frame in Fig. 5(b) as primary, denoted $p(m,n)$ below, and the LWIR frame of Fig. 5(a) as reference, denoted $r(m,n)$. The filter output is given by $y(m,n) = p(m,n) - w_{m,n} r(m,n)$, where

$$w_{m,n} = \frac{\sum_{i=-N}^{N} \sum_{j=-N}^{N} p(m+i,n+j) r(m+i,n+j)}{\sum_{i=-N}^{N} \sum_{j=-N}^{N} r(m+i,n+j) r(m+i,n+j)}$$

is an estimate of the correlation between the bands in a $(2N+1) \times (2N+1)$ pixel window about the pixel site (m,n). Results of applying the color filter to the frame pair in Fig. 5(a) and (b) with $N = 2$ are given in Fig. 5(c), where an appreciable reduction of the clutter has been achieved.

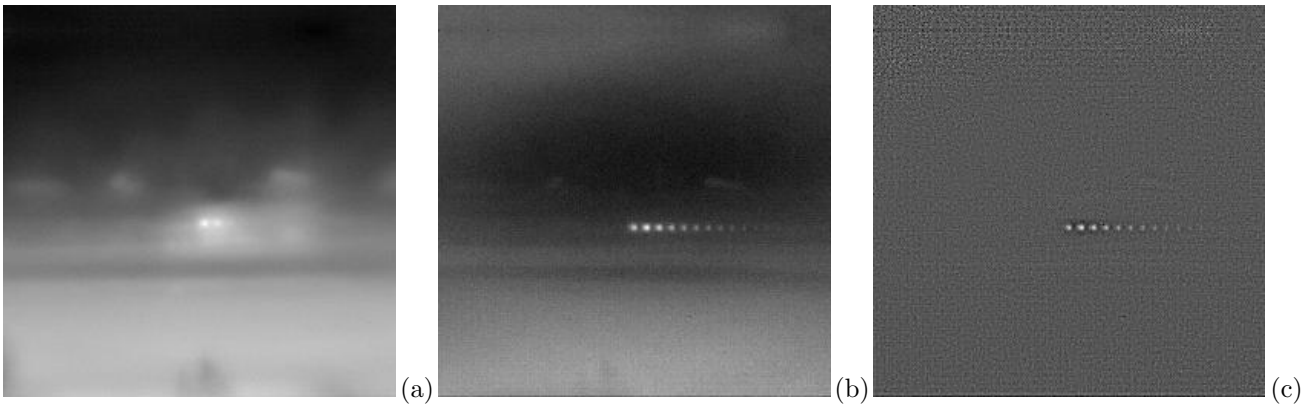

Figure 5. Another example showing dual-band imagery with data fusion. (a) Sport utility vehicle in the LWIR band. (b) Sport utility vehicle in the MWIR band; significant temporal aliasing is visible. (c) Spectral correlation filter result: weighted subtraction of the LWIR band from the MWIR band. The weights, which are computed on a pixel-by-pixel basis, are local estimates of the correlation coefficient between bands computed over 5×5 neighborhoods.

5. SENSOR ISSUES

Operated at broadband with our 50 mm, $f/1.0$, $18^\circ \times 13.5^\circ$ FOV optics, the PV320L2Z generally produces clear, uniform imagery not dissimilar in appearance from the longwave frame shown in Fig. 4(d). With the midwave and longwave warm filters in place, however, it has not always been possible to obtain consistently good imagery, particularly in the 3–5 μm band. When the ambient temperature is above 30° C, we have generally been successful in acquiring dual-band imagery such as that shown in the examples of Section 4. However, at ambient temperatures below 20° C, we have encountered considerable difficulty. One such example is shown in Fig. 6. This is an LWIR image taken with the 8–12 μm filter in place. The scene consists of a person holding a weak flashlight. The ambient temperature was 20° C and the range to target was approximately 5 m. Although this image was acquired with manual sensitivity, level, and gain settings, the results obtained with autoexposure were not significantly different. It should be noted that this image was acquired using the default factory preset non-uniformity correction. While it is very likely that this NUC is less than optimal when imaging in reduced spectral bands, we are skeptical that an improved calibration scheme would be able to fully resolve all of the problems apparent in Fig. 6. Since upgraded optics and/or focal plane array technologies are not currently within the realm of budgetary possibilities for this project, we plan to focus our future data acquisition efforts in the late summer months where sufficient ambient temperatures can be expected.

6. CONCLUSION

This paper described the integration of a low-cost dual-band infrared imaging system constructed around a pair of Electrophysics PV320L2Z uncooled broadband BST array cameras. The main goal of the project is to acquire dual-band MWIR/LWIR imagery that can be used for unclassified target detection and recognition research. This is significant in view of the general paucity of such data in the public domain. Because the cameras were not designed for use in a dual-band system, several significant technical challenges had to be overcome in order to make the system operational. We described in some detail the software design that was required to operate the two cameras simultaneously and acquire temporally registered frame pairs. Ultimately, a pair of identical laptop computers were required to control the cameras individually and a client-server software architecture was developed to enforce lock step synchronization between the server side and client side applications.

Using warm filters inserted between the lens and camera chopper wheel, we typically operate one camera in the midwave $3 - 5$ μm band and the other in the longwave $8 - 12$ μm band. These filters are inexpensive and easily interchangeable, suggesting that a variety of narrow bandpass filters could be used to perform dual-band data fusion experiments between a large number of choices of operational bands. In practice, however, the problems we encountered with low SNR and sensitivity even in the relatively wide $3 - 5$ μm and $8 - 12$ μm bands suggest that this approach is impractical with our current optics and detector technology.

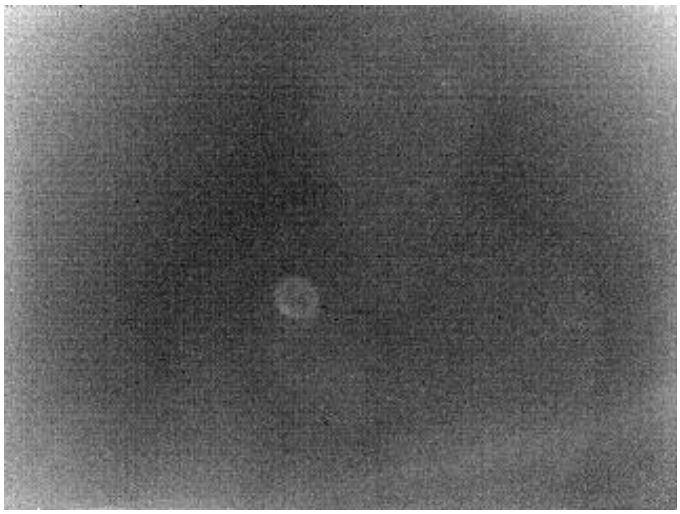

Figure 6. Example of poor signal to noise ratio obtained in a longwave (8 – 12 μm) frame acquired at an ambient temperature of 20° C. The scene is of a person holding a weak flashlight. Range to target is approximately 5 m.

Nevertheless, the examples presented in Section 4 demonstrate that the system is capable of delivering reasonably high quality dual-band imagery of scenes including, e.g., typical vehicles and backgrounds in ambient temperatures above 30° C. We obtained dual-band fusion results using both simple addition of the MWIR and LWIR frames and a spectral correlation filter. Currently, we are planning an aggressive data acquisition schedule for summer, 2006.

ACKNOWLEDGMENTS

This work was supported in part by the U.S. Army Research Laboratory and the U.S. Army Research Office under grant W911NF-04-1-0221.

REFERENCES

1. A. Goldberg, T. Fischer, and Z. Derzko, "Application of dual-band infrared focal plane arrays to tactical and strategic military problems," in *Infrared Technology and Applications XXVIII*, B. Andersen, G. Fulop, and M. Strojnik, eds., *Proc. SPIE* **4820**, pp. 500–514, 2003.
2. R. Breiter, W. Cabanski, K.-H. Mauk, W. Rode, J. Ziegler, H. Schneider, and M. Walther, "Multicolor and dual-band IR camera for missile warning and automatic target recognition," in *Targets and Backgrounds VIII: Characterization and Representation*, W. Watkins, D. Clement, and W. Reynolds, eds., *Proc. SPIE* **4718**, pp. 280–288, 2002.
3. R. McDaniel, D. Scribner, W. Krebs, P. Warren, N. Ockman, and J. McCarley, "Image fusion for tactical applications," in *Infrared Technology and Applications XXIV*, B. Andresen and M. Strojnik, eds., *Proc. SPIE* **3436**, pp. 685–695, 1998.
4. N. Gupta and D. Smith, "A simultaneous dual-band infrared hyperspectral imager for standoff detection," in *Chemical and Biological Standoff Detection III*, J. Jensen and J. Thériault, eds., *Proc. SPIE* **5995**, pp. 5995OL–1 – 5995OL–10, 2005.
5. A. Goldberg, T. Fisher, S. Kennerly, S. Der, A. Chan, M. Lander, C. Garvin, S. Wang, M. Falco, D. Campagna, and A. Costillo, "Analysis of dual-band infrared imagery from the multidomain smart sensor field test," Tech. Rept. ARL-TR-996, Army Research Laboratory, Adelphi, MD, Jun. 2002.
6. P. Dainty, J. F. Boyce, C. H. Dimitropoulos, P. Edmundson, D. L. Toulson, and M. Bernhardt, "Dual-band ATR for forward-looking infrared images," in *Proc. IEEE Workshop Comput. Vision Beyond Visible Spectrum*, pp. 23–29, Jun. 21-22 1999.

7. L. A. Chan, S. Z. Der, and N. M. Nasrabadi, "Dual-band passive infrared imagery for automatic clutter rejection," in *Proc. IEEE Int'l Conf. Image Proc.*, pp. 463–466, (Vancouver, Canada), Sep. 10-13 2000.
8. M. Smith and J. Heather, "Review of image fusion technology in 2005," in *Thermosense XXVII*, G. Peacock, D. Burleigh, and J. Miles, eds., *Proc. SPIE* **5782**, pp. 29–45, 2005.
9. J. P. Havlicek, P. C. Tay, and A. C. Bovik, "AM-FM image models: Fundamental techniques and emerging trends," in *Handbook of Image and Video Processing*, A. C. Bovik, ed., pp. 377–395, Elsevier Academic Press, Burlington, MA, 2nd ed., 2005.
10. J. P. Havlicek, D. S. Harding, and A. C. Bovik, "Multidimensional quasi-eigenfunction approximations and multicomponent AM-FM models," *IEEE Trans. Image Proc.* **9**, pp. 227–242, Feb. 2000.
11. T. Peli, P. Monsen, R. Stahl, M. Pauli, and K. McCamey, "Signal processing improvements for infrared missile warning sensors," in *Proc. IEEE Nat'l. Aerospace, Electronics Conf.*, pp. 1052–1064, Jul. 14-17 1997.